ANNALS OF GEOPHYSICS, 59, Fast Track 5, 2016; DOI: 10.4401/ag-7182

Preliminary engineering analysis of the August 24th 2016, M_L 6.0 central Italy earthquake records

IUNIO IERVOLINO [1], GEORGIOS BALTZOPOULOS [2], EUGENIO CHIOCCARELLI [2]

[1] Dipartimento di Strutture per l'Ingegneria e l'Architettura, Università degli Studi di Napoli Federico II, Italy.

iunio.iervolino@unina.it

[2] Construction Technologies Institute ITC-CNR, URT at Dipartimento di Strutture per l'Ingegneria e l'Architettura, Università degli Studi di Napoli Federico II, Italy.

baltzopoulos@itc.cnr.it; chioccarelli@itc.cnr.it

Abstract

An earthquake of estimated local magnitude (M_L) 6.0 struck central Italy on the 24th of August (01:36:32 UTC) in the vicinity of Accumoli (close to Rieti, central Italy) initiating a long-lasting seismic sequence that also featured events of larger magnitude within a few months. The earthquake caused widespread building damage and around three-hundred fatalities. Ground motion was recorded by hundreds of seismic stations. This work uses accelerometric records for a preliminary discussion, from the earthquake engineering perspective, of strong motion caused by the earthquake. Peak and integral ground motion intensity measures, are presented. The response spectra at some select stations are analysed with respect to the code-mandated design actions for various return periods at the recording sites. Hazard disaggregation for different return periods is discussed referring to the site of the epicentre of the earthquake. Finally, some preliminary considerations are made concerning the impact of rupture propagation on near-source ground motion; i.e., the records are scanned for traces of pulse-like forward-directivity effects.

I. INTRODUCTION

The national accelerometric network of Italy (RAN), operated by the governmental *Dipartimento delle Protezione Civile* (DPC), and the Italian seismic network (RSN), operated by the *Istituto Nazionale di Geofisica e Vulcanologia* (INGV) have made available, rapidly after the event, the records of the earthquake, with epicentre located in the vicinity of Accumoli, central Italy, that struck on Aug. 24 2016, at 1:36:32 AM – UTC. The moment magnitude (M_w) declared by INGV is 6.0, while other international institutions claim M_w 6.2. Corrected records and processing details are available on the *Engineering Strong-Motion database* website, while the uncorrected waveforms can be found on the RAN and RSN websites (see section VI).

The present short article deals with some aspects of recorded strong ground motion of earthquake engineering interest. First, shaking intensity parameters for some of the ground motions recorded nearest to the fault are presented. Then, response spectra for some of the stations closer to the source are compared to the code-mandated spectra. Finally, near-source ground motions are examined for impulsive characteristics to be possibly attributed to rupture directivity.

II. GROUND MOTION INTENSITY MEASURES AND RESPONSE SPECTRA

Table 1 shows some peak and integral ground motion intensity measures (IMs) for the records within 30km from the source (i.e., Joyner-and-Boore distance, R_{jb}). More specifically, data reported in the table are: the ID of the station, the R_{jb} distance, the soil class[1] according to the code (CS.LL.PP. 2008, NTC2008 hereafter), the peak ground acceleration of the east-west horizontal component (PGA_E), and of the north-south component (PGA_N), the angle with respect to the north (positive clockwise) to which corresponds the maximum recorded PGA $\left(\theta_{PGA}\right)$, the corresponding PGA (Max PGA). The maximum pseudo-acceleration response spectrum ordinate at 0.3s and 5% damping, $Sa(0.3)$, is given in the same table along with the angle to which it corresponds; i.e., Max $Sa(0.3)$ and $\theta_{Sa(0.3)}$, respectively. The same information is provided, with analogous notation, assuming an oscillation period of 1.0s. Considered integral parameters are the *Arias intensity* (IA) and the significant duration $\left(D^{5-95}\right)$ for the horizontal components, estimated between 5% and 95% of IA. Finally, if available, vertical PGA values are also reported (PGA_V).[2]

Data reported in Table 1 show that MAX PGA and $Sa(0.3)$ recorded by NRC and AMT station were significantly higher than those recorded by all the other stations, while the highest Max $Sa(1.0)$ was recorded by the NOR station. In particular, PGA_E of the AMT station is the highest horizontal PGA recorded up to that point in Italy (larger PGAs may have occurred later in the sequence, yet this is not yet fully consolidated).

Among other stations, a few records have values somewhat departing from the general trend: FEMA, CLF, FOC and TRE if PGA and $Sa(0.3)$ are considered, and RM33 and CLF if $Sa(1.0)$ is of concern (see also Section IV). A similar situation applies to integral parameters.

To have a more complete picture of the characteristics of the recorded IMs, these have to be compared with ground motion prediction equations (GMPEs). One of such comparison can be found in ReLUIS-INGV Workgroup (2016a), that also includes the complete response spectra (elastic and inelastic) for the

[1] Asterisks indicate that soil classification is based on inferred, rather than measured, average shear velocity in the upper 30m.

[2] IMs from AMT station are derived from the revised records provided by RAN website several weeks after the event. Moreover, at the time of the submission of this paper, recordings from AQA and NOR stations have been retracted pending possible revision by the DPC. AQA and NOR data analysed here are those available prior to said revision.

records considered here, as well as for others more distant from the source. Another comprehensive comparison of observed ground motion peak parameters and predicted IMs is provided in Lanzano et al. (2016) with respect to two different GMPEs. In that paper, it is underlined that the GMPEs generally fit the observations for low spectral periods and short source-to-site distances and seem to underpredict the observed IMs at distances larger than 80 km.

III. THE RECORDS AND THE ITALIAN SEISMIC CODE

In Figure **1** the pseudo-acceleration response spectra associated to the horizontal ground motions, recorded by some of the stations with the smallest R_{jb} distance, are compared with the elastic design spectra provided by the Italian building code, at the corresponding sites, for four different return periods (T_R): 50, 475, 975 and 2475 years.

Before proceeding any further, it is worthwhile recalling that NTC2008 spectra are a direct approximation of the uniform hazard spectra computed via the probabilistic seismic hazard analysis (PSHA) discussed in Stucchi et al. (2011).

The east-west component of AMT exceeds the 2475 years spectra in the 0s-0.4s range of periods, while at least one component of the same station exceeds the 475 years spectra for spectral periods up to 2.1s. NRC and FEMA (see Figure 2a, for the position with respect to the source) exceed the 475 years spectra in the range of periods 0s-0.3s and 0.35s-0.5s respectively. This applies to at least one of the two horizontal components (for NRC record, the exceedance happens also for 0.67s-0.88s). The NRC record also exceeds the 2475 years spectrum for periods between 0.13s and 0.28s. However, at all the stations for longer oscillation periods, and as soon as the distance increases, spectral ordinates become comparable with code-spectra corresponding to return periods of a few tens of years.

The maximum ratios of the peak of the pseudo-acceleration spectrum (5% damping) and the PGA are equal to 5.1 and 2.7, for NRC and AMT stations, respectively (these refer to the east-west and north-south directions without investigating other possible rotations). Notwithstanding the not completely intelligible (so far at least) differences between the two horizontal components of AMT, the shape and the amplitude of these spectra appear compatible with extensive damage in some villages, where the population of structures suffered significant damage or total collapse.

It should be also discussed that exceedance of code spectra close to the source of a strong earthquake does not directly imply inadequacy of PSHA at the basis of the code spectra (Iervolino, 2013). This is also because spectra from PSHA, are the results of an average of a series of scenarios considered possible (e.g., small and large source-to-site distances). Such an average may be exceeded close to the source of an earthquake, even if the corresponding scenario is included in the PSHA.

Referring to the coordinates of the epicentre (42.70N; 13.24E), the hazard disaggregation (e.g., Iervolino et al., 2011) was computed, by means of REXEL v 3.5 (Iervolino et al., 2010), for PGA and for $Sa(1.0)$, for two return periods (475 and 2475 years). The entire set of disaggregation distributions is not shown here for the sake of brevity (although it can be found in

ReLUIS-INGV Working group, 2016a). Nevertheless, the relevant scenarios for the considered return periods and IMs are summarized here; they are the magnitude and distance intervals that have probability, of being causative for the exceedance of the corresponding IM, larger than 0.5. All of these scenarios are characterized by the same distance range between 0km - 20km. Magnitude intervals for *PGA* are 5.3 - 6.3 and 5.9 – 6.8 for 475 years and 2475 years, respectively. For $Sa(1.0)$, and the same return periods, magnitude intervals are 6.0–7.0 and 6.3-7.0, respecitively. It may be concluded that, according to the hazard analysis the code is based on, exceedance of high-frequency spectral accelerations, corresponding to 475 years and 2475 years T_R, is most likely caused by a close moderate-magnitude earthquake that is loosely compatible to what was observed.

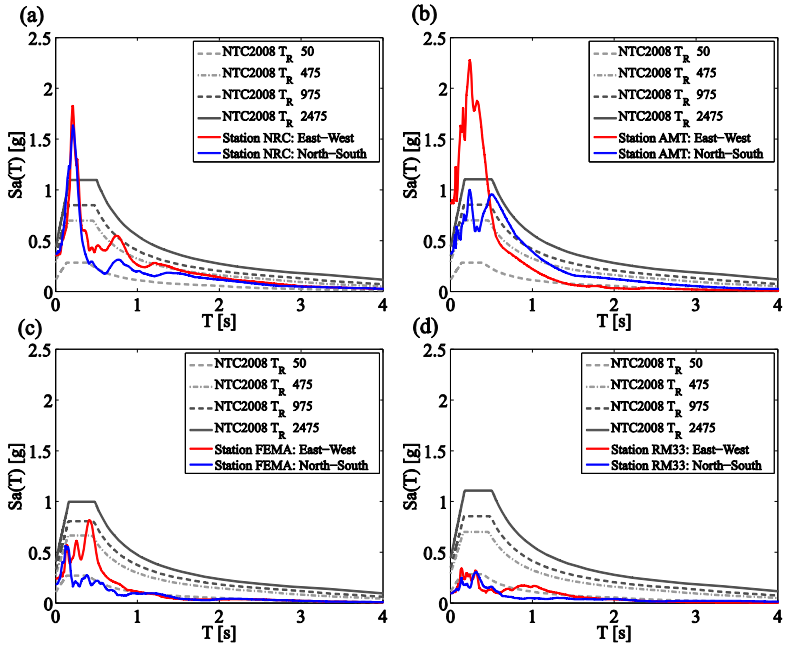

Figure 1. Comparison between the observed ground motions and the elastic design spectra provided by NTC2008.

IV. Analysis of pulse-like directivity effects

Pulse-like near-source (NS) ground motions may be the result of rupture directivity. This can lead to a constructive wave interference effect, which is manifested in the form of a double-sided velocity pulse that delivers most of the seismic energy early in the record (Somerville et al., 1997). Clues of impulsive features in near-source ground motions have been probably found in Italian seismic events of normal faulting style before (e.g., Chioccarelli and Iervolino, 2010). In this preliminary investigation for such pulse-like effects, the continuous wavelet transform algorithm suggested by Baker (2007) was implemented for all recordings (horizontal components) within a closest-to-rupture distance of 30km from the fault and for all orientations.

It should be noted that the adopted approach is purely phenomenological, extracting empirical evidence of impulsive characteristics directly from the recorded NS signals without attempting to assign a causal relation to specific effects falling under the banner of rupture directivity (i.e., rupture propagation, seismic source radiation pattern, motion polarization). Models regarding the phenomenon through the prism of the physics of finite-fault rupture are also available (e.g., Spudich and Chiou, 2008) but not followed in this preliminary analysis.

The surface projection of the fault rupture plane (Tinti et al., 2016) is shown in Figure 2a along with the equal-probability contours of the Iervolino and Cornell (2008) model for the probability of observing NS directivity pulses. It can be observed that, interestingly enough, some of the most prominent impulsive waveforms (NRC, NOR, FEMA, RM33) have been recorded at sites where the empirically-calibrated model assigns low probability of pulse occurrence due to directivity. This is indicative of the fact that more research is required into the phenomenon for the case of normal faulting, but it should also be mentioned that there were hardly any accelerometric stations present in the area where pulse-like effects were most probable to be observed according to the model.

Out of all the records investigated, six ground motions exhibited impulsive characteristics, as expressed by a Pulse Indicator (PI) score in excess of 0.85 (see Baker, 2007). The AMT record revealed two distinct pulses. One with pulse period T_p of 0.41s being predominant in the fault-normal (FN) and another, longer duration pulse with T_p = 0.98s in the fault-parallel (FP) direction (Figure 2b). The latter might be attributed to the breakage of a nearby asperity on the fault plane (Tinti et al., 2016). The FEMA record was also discovered to exhibit impulsive characteristics in both FN (T_p = 0.50s) and FP directions. The ground motions recorded at the MNF station and RM33 were found to contain pulses in the FN direction (T_p = 1.40s and 1.20s respectively) that also hinted at rupture directivity effects, despite the lower velocity amplitude due to the greater distance from the fault and consequent attenuation. This leaves the two ground motions recorded at Norcia, NRC and NOR, that were of particular interest. The NRC record was found to contain a 2.09s period pulse mostly towards orientations that lie between the FN and FP but somewhat more prevalent in the direction perpendicular to the strike. Interestingly, it is known that the NRC site sits upon deep soil deposits characterized by an inversion of velocity profile at a depth of more than 30m (see Bindi et al., 2011) and this cannot be disregarded when narrow-band characteristics are observed in the recordings. However, station NOR was also found to be pulse-like, with a 1.63s pulse in the FN direction (see Figure 2c). Furthermore, records obtained at the base/ground-level of instrumented, seismically monitored buildings distant up to 500m from the two accelerometric stations, contained velocity pulses almost identical in orientation and period to the NOR station. This consistency enhances the argument in favour of the presence of a directivity effect.

One prominent characteristic of directivity-induced velocity pulses is that they tend to

dominate the spectral shape of the signal's pseudo-velocity spectrum. This is also confirmed in the case examined here; see Figures 2(d-e). Furthermore, pulse period T_p (as defined via the wavelet transform, see Baker, 2007) is very well correlated with predominant ground motion period T_g (vibration period where maximum pseudo-velocity occurs); also confirmed in this case. Note that the extracted pulses typically correspond to some local maximum also on the pseudo-acceleration spectrum (Sa), but do not necessarily account for the absolute maximum amplitude, which is usually determined by the higher-frequency content.

Finally, when the pulse periods extracted from the various NS sites examined are compared against the empirical regression model from Baltzopoulos et al. (2016), they are found in reasonable agreement with what is expected for a M_w 6.0 event (T_p geometric mean of 1.02s compared to predicted median of 1.29s).

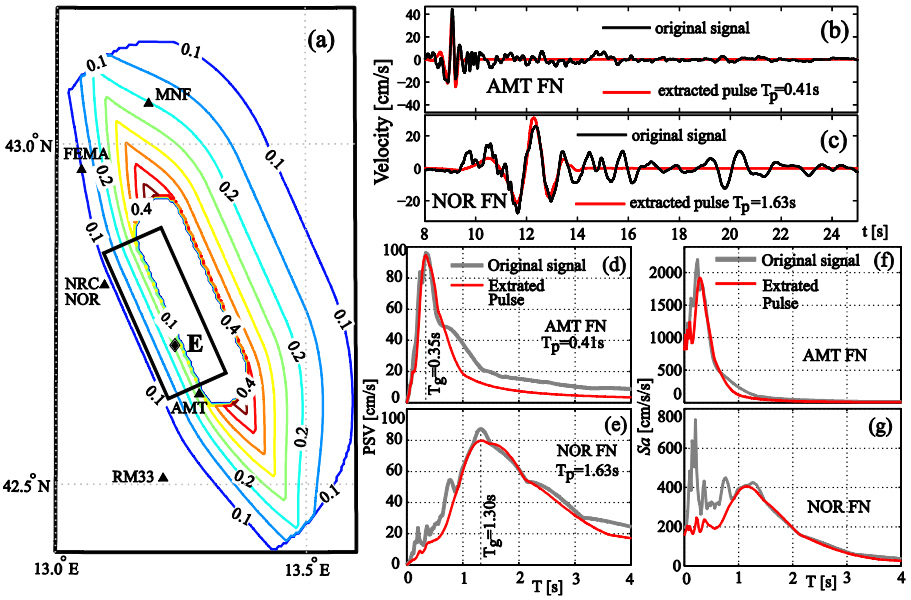

Figure 2. Equal probability of pulse occurrence contours, according to the model of Iervolino and Cornell (2008), plotted against the surface projection of the rupture plane (a), velocity time-history and extracted pulse of AMT FN component (b) and NOR FN (c), pseudo-velocity spectra (PSV) of the extracted pulses plotted against PSV of the original signal for the FN components of AMT (d) and NOR (e), pseudo-acceleration spectra of the extracted pulses plotted against Sa of the original signal for the FN components of AMT (f) and NOR (g).

V. CONCLUSIONS

This article provided a preliminary engineering-point-of-view analysis of the strong motion records obtained during the Amatrice earthquake that struck central Italy on 24th of August 2016. An overview of the ground motion intensity parameters typically associated with structural response was given, identifying stations with highest IMs, with AMT exhibiting the highest horizontal PGA recorded

in Italy so far. The comparison of some of the closest-to-rupture records' spectra and the code spectra showed cases of exceedance of the latter by the former at T_R 475 years and even T_R 2475 years. It was then briefly discussed how this is to be expected, even though to claim otherwise can be a common pitfall. Finally, it can be said that some indications of pulse-like NS motions were observed, which could be the result of rupture directivity. Points of interest that merit further investigation include the potential role of site effects in the manifestation of some particular spectral shapes and the juxtaposition of inelastic response spectra with damages.

VI. Postscript

This paper was prepared before the occurrence of other large earthquakes from same seismic sequence. Indeed, since the first submission of this article, two further strong earthquakes have struck the area, the 26/10/2016 M_w 5.9 Ussita event and the 30/10/2016 M_w 6.5 Norcia event. As such, the 24/08 M_w 6.0-6.2 Amatrice earthquake is currently regarded as the initiating event of the long-lasting 2016 central Italy sequence, with the Norcia seismic event being typically nominated as the overall mainshock, so far. Herein the first event was discussed, while the reader is referred to ReLUIS-INGV Workgroup (2016b) for a more comprehensive analysis of the sequence as a whole.

VII. Data and sharing resources

Records used herein were processed and provided to the authors by the ITACA-ESM Working Group of the Istituto Nazionale di Geofisica e Vulcanologia (INGV). They are also available at http://esm.mi.ingv.it/ (last accessed 21/11/2016).

The unprocessed records can be accessed at http://ran.protezionecivile.it for the RAN network and at the European Integrated Data Archive (http://www.orfeus-eu.org/data/eida/) for the RSN.

The parameters of the finite-fault geometry used are available at http://esm.mi.ingv.it and are attributed to Tinti et al. (2016).

Accelerograms recorded at the monitored structures in Norcia are available from the Seismic Observatory of Structures of the National Civil Protection – www.mot1.it.

VIII. Acknowledgments

The study presented in this paper was developed within the activities of ReLUIS (*Rete dei Laboratori Universitari di Ingegneria Sismica*).

IX. References

Baker J.W. (2007). Quantitative Classification of Near-Fault Ground Motions Using Wavelet Analysis. Bull. Seismol. Soc. Am., 97(5):1486–1501.

Baltzopoulos G., D. Vamvatsikos and I. Iervolino (2016). Analytical modelling of near-source pulse-like seismic demand for multi-linear backbone oscillators. Earth. Engin. Struct. Dyn., 45(11):1797–1815.

Bindi D., L. Luzi, S. Parolai, D. Di Giacomo and G. Monachesi (2011). Site effects observed in alluvial basins: the case of Norcia (central Italy). Bull. Earthquake Eng., 9:1941-1959.

Chioccarelli E., I. Iervolino (2010). Near-Source Seismic Demand and Pulse-Like Records: a Discussion for L'Aquila Earthquake. Earthq. Engn. Struct. Dyn., 39(9):1039–1062.

CS.LL.PP. (2008). Decreto Ministeriale 14 gennaio 2008: Norme tecniche per le costruzioni. Gazzetta Ufficiale della Repubblica Italiana, 29 (in Italian).

Iervolino I., C.A. Cornell (2008). Probability of occurrence of velocity pulses in near-source ground motions. Bull. Seismol. Soc. Am., 98(5):2262-2277.

Iervolino, I. (2013). Probabilities and fallacies: why hazard maps cannot be validated by individual earthquakes. Earthq. Spectra, 29(3):125–1136.

Iervolino, I., C. Galasso and E. Cosenza (2010). REXEL: computer aided record selection for code based seismic structural analysis. Bull. Earthq. Eng., 8:339-362.

Iervolino, I., E. Chioccarelli and V. Convertito (2011). Engineering design earthquakes from multimodal hazard disaggregation. Soil Dyn. Earthq. Eng., 31:1212-1231.

Lanzano G., L. Luzi, F. Pacor, R. Puglia, M. D'amico, C. Felicetta and E. Russo (2016). Preliminary analysis of the accelerometric recordings of the August 24th, 2016 M_w 6.0 Amatrice earthquake. Annals of Geophysics, 59, Doi: 10.4401/ag-702.

ReLUIS-INGV Workgroup (2016a). Preliminary study of Rieti earthquake ground motion records V5, available at http://www.reluis.it.

ReLUIS-INGV Workgroup (2016b). Preliminary study on strong motion data of the 2016 central Italy seismic sequence V6, available at http://www.reluis.it.

Somerville P.G., N.F. Smith, R.W. Graves and N.A. Abrahamson (1997). Modification of empirical strong ground motion attenuation relations to include the amplitude and duration effects of rupture directivity. Seismol. Res. Lett., 68:199–222.

Spudich, P., B.S.J. Chiou (2008). Directivity in NGA earthquake ground motions: analysis using isochrone theory. Earthq. Spectra 24(1): 279-298.

Stucchi, M., C. Meletti, V. Montaldo, H. Crowley, G.M. Calvi and E. Boschi (2011). Seismic hazard assessment (2003–2009) for the Italian building code. B. Seismol. Soc. Am., 101:1885–1911.

Tinti, E., L. Sconamiglio, A. Michelini and M. Cocco (2016). Slip heterogeneity and directivity of the M_L 6.0, 2016, Amatrice earthquake estimated with rapid finite-fault inversion. Geophys. Res. Lett., 43(10): 10,745-10,752.

Table 1. IMs of the recorded ground motions within 30 km from the source (distance in terms of R_{jb}).

Station ID	Soil Class	R_{jb} [km]	PGA_E [g]	PGA_N [g]	θ_{PGA} [°]	Max PGA [g]	$\theta_{Sa(0.3)}$ [°]	Max $Sa(0.3)$ [g]	$\theta_{Sa(1.0)}$ [°]	Max $Sa(1.0)$ [g]	IA_E [cm/s]	D_E^{5-95} [s]	IA_N [cm/s]	D_N^{5-95} [s]	PGA_V [g]
AMT	B*	1.4	0.867	0.376	90	0.867	96	1.833	13	0.400	188.52	3.74	72.23	3.16	0.399
NRC	B	2.0	0.359	0.373	145	0.452	138	0.897	100	0.267	104.37	6.00	82.59	6.25	0.216
NOR	C*	2.3	0.202	0.180	48	0.203	141	0.474	87	0.405	55.95	10.27	34.33	17.02	-
MMO1	A*	9.7	0.118	0.139	154	0.149	129	0.442	161	0.127	7.12	7.13	19.40	9.05	-
RM33	B*	13.0	0.102	0.101	104	0.106	53	0.356	93	0.170	8.66	8.64	6.07	9.13	0.036
FEMA	B*	13.9	0.247	0.189	84	0.248	103	0.444	92	0.116	30.49	5.02	12.42	7.68	-
SPD	B*	16.1	0.053	0.102	9	0.103	2	0.204	53	0.117	3.95	10.39	7.16	8.62	0.055
MNF	A*	20.4	0.073	0.044	69	0.078	56	0.150	89	0.069	3.03	6.86	1.48	10.91	0.061
TERO	B*	22.1	0.057	0.085	176	0.085	79	0.122	131	0.036	4.70	11.22	7.50	9.75	0.036
LSS	A	22.2	0.022	0.018	112	0.024	53	0.080	37	0.016	0.74	16.72	0.67	18.90	0.015
PZI1	B*	22.7	0.045	0.046	58	0.052	23	0.161	88	0.062	2.38	11.63	2.87	14.89	0.026
ANT	A*	26.0	0.014	0.024	25	0.026	20	0.062	4	0.059	0.68	25.19	1.13	20.96	0.009
CLF	D	26.1	0.125	0.131	129	0.142	165	0.456	29	0.198	18.13	9.03	14.11	10.80	0.105
FOC	C*	26.3	0.261	0.329	20	0.351	104	0.522	156	0.029	36.24	5.60	38.48	4.22	0.128
FOS	B*	28.8	0.060	0.076	40	0.090	31	0.230	92	0.039	4.64	9.02	5.94	8.81	0.041
AQF	B*	29.3	0.044	0.038	92	0.044	174	0.161	99	0.024	1.96	12.03	1.71	14.96	0.033
AQV	B	29.3	0.061	0.046	84	0.061	127	0.103	112	0.065	3.00	14.23	2.82	15.89	0.023
AQA	E	29.4	0.002	0.002	2	0.002	45	0.005	102	0.003	0.00	14.86	0.01	14.94	0.001
TRE	C*	29.6	0.064	0.111	33	0.118	39	0.276	27	0.097	5.10	14.62	10.62	14.52	0.046
TRL	A*	30.2	0.036	0.039	164	0.041	47	0.095	33	0.047	2.58	20.84	3.79	20.28	0.018
GSA	B	30.7	0.036	0.037	110	0.038	66	0.071	53	0.020	1.37	17.12	1.75	15.33	0.019
SPM	A*	30.9	0.067	0.065	98	0.068	38	0.104	18	0.030	4.93	14.43	4.99	12.48	0.021